ECAP-2018-007

Bachelor Thesis

Temperature Measurement of Silicon Photomultipliers via Calibrated IV Characteristics

submitted by
Naomi Vogel
April 9, 2018

Supervised by: PD Dr. Thilo Michel
Erlangen Centre for Astroparticle Physics
Friedrich-Alexander-Universität Erlangen-Nürnberg

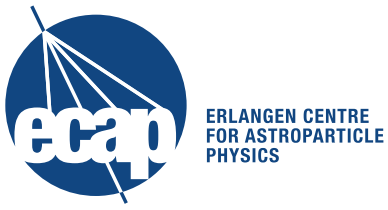

Contents

1 Introduction

Over the past years development has taken place in the field of semiconductor photodetectors. With Silicon Photomultipliers (SiPM), pixelated semiconductor photodetectors, an alternative to photomultiplier tubes (PMT) has been provided. In comparison to PMTs, SiPMs have several advantages such as operation at low bias ($< 100\,\mathrm{V}$), insensitivity to magnetic fields, low power consumption, single-photon resolution, compactness and robustness. They are manufactured at low cost and can be reproduced easily [1]. SiPMs consist of an array of single avalanche photodiodes (APD) connected in parallel and operated in Geiger mode, therefore achieving a gain of about 10^5 to 10^6 [1]. Several parameters of SiPMs have been established, e.g. dark noise rate, crosstalk, afterpulsing and photon detection efficiency. These characteristic parameters as well as the breakdown voltage and cut-in voltage are temperature-dependent. For this reason, knowing the precise temperature at which a SiPM is operated is crucial for all characterization efforts.

The goal of a setup operated at the Erlangen Centre for Astroparticle Physics (ECAP) is to characterize vacuum ultraviolet (VUV)-sensitive SiPMs. The setup is planning to use liquid xenon (LXe) whose scintillation light is in the VUV range. Precisely for these characterization efforts it is essential to know the accurate temperature of the SiPM. Because its surface is easily scratched and needs to be photosensitive it is impossible to apply a temperature sensor directly to the SiPM. The sensor can only display the temperature of the surroundings.

In this thesis a method using a SiPM as a thermometer by deriving its temperature directly from the diode IV-characteristics is developed. In advance the diode IV-characteristics for various temperatures need to be calibrated under controlled ambient conditions.

2 Theoretical Background

2.1 Silicon Photomultipliers

Silicon photomultipliers (SiPMs) are semiconductor photodetectors with single-photon resolution. They are built out of multiple single avalanche photodiodes (APD) connected in parallel that are operated in Geiger mode.

An APD is a p-n device. The term p-type semiconductor refers to the addition of a trivalent impurity to a tetravalent semiconductor, e.g. adding boron to silicon. This leads to a large number of holes. In contrast, the term n-type semiconductor refers to the addition of a pentavalent impurity to a tetravalent semiconductor, e.g. adding phosphorus to silicon. This, in turn, leads to a large number of weakly bound electrons. This structure is shown in figure 2.1 where the red circles represent the free electrons and the gray circles the holes. When joining these two semiconductor types, a p-n junction is formed. A diffusion of charge carriers is registered at the junction because the electrons in the n-layer move from their high concentration region towards the p-layer acting as the low concentration region, whereas the holes of the p-layer move towards the n-layer. Due to this diffusion, recombination of the holes and electrons takes place. Negative ions are formed in the p-layer and positive ions are formed in the n-layer near the junction. After this process, the n-layer is positively charged while the p-layer is negatively charged. These net charges prevent more free electrons or holes from crossing the junction, acting as a negative and positive barrier. This barrier is also called the depletion region because of its low concentration of free charge carriers. Minority charge carriers are still able to cross the junction so that an equilibrium can be reached. [2]

When looking at a semiconductor diode, external voltage, also called bias, is applied in an either forward or reverse direction. In order to allow a current flow, the p-type is connected to the positive terminal and the n-type to the negative terminal, which results in forward biasing and is shown on the left in figure 2.2. When forward bias is increased, the depletion region is decreased, allowing a negligible electric current to flow, the so called leakage current. If the voltage is increased even more the depletion region is further reduced, resulting in a rapid increase in electric current.

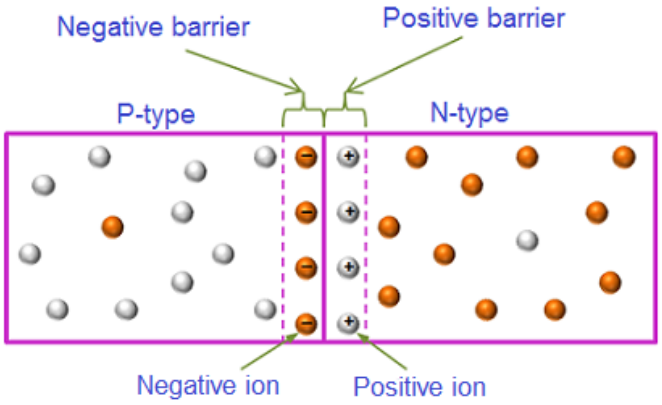

FIGURE 2.1: Schematic structure of a p-n junction. The red circles represent the free electrons and the gray circles the holes. Due to diffusion of charge carriers, negative ions are formed in the p-layer and positive ions in the n-layer, acting as a potential barrier. Both barriers together are also called the depletion region. [2]

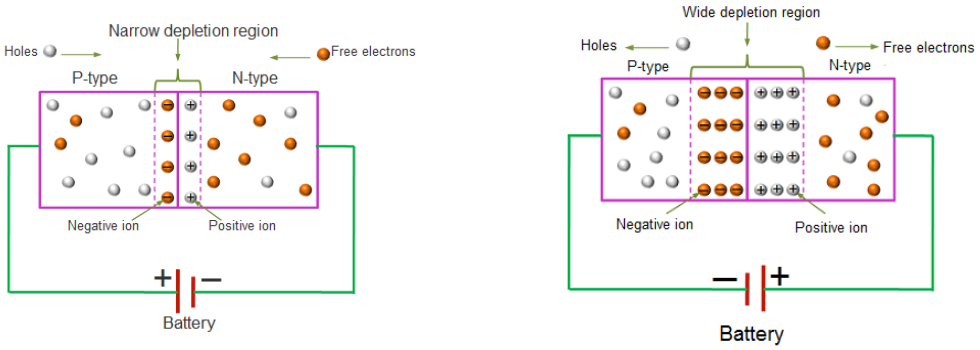

FIGURE 2.2: On the left a schematic layout of applying forward bias to a p-n device is shown. The depletion region is reduced with increasing voltage. On the right a schematic layout of applying reverse bias to a p-n device is shown. The depletion region expands with increasing voltage. [2]

Accordingly, the depletion region of a diode decreases when voltage is increased. For reverse biasing, shown on the right in figure 2.2, the p-type is connected to the negative terminal and the n-type to the positive terminal. Holes from the p-layer are attracted to the negative terminal and are filled with electrons. Similarly, free electrons from the n-layer are attracted to the positive terminal. The formed ions block the flow of majority charge carriers. When increasing the reverse bias, the depletion width expands because more free electrons and holes are pulled away from the p-n junction. However, it's possible for minority charge carriers to carry a negligible current in reverse bias. [2]

An avalanche diode is a special semiconductor diode operated above reverse breakdown region. When increasing the applied external voltage in reverse direction, a steady gain of electrical current is registered. The voltage at which the current increases rapidly is called breakdown voltage. After exceeding this voltage, the junction breaks down, which is referred to as the avalanche breakdown. When forward bias is applied to the diode, electric current is able to flow. [2]

Avalanche photodiodes belong to the group of avalanche diodes and convert absorbed photons into electric pulses. An APD is a p-n device which is based e.g. on a p^+-i-p-n^+ dopant profile. The basic structure of an APD with the avalanche breakdown process and the diode's electrical field is shown in figure 2.3. It consists of a highly doped p^+-layer followed by a large intrinsic layer i which is supposed to absorb an incoming photon via the inner photoelectric effect creating an electron hole pair. The photon's entire energy is transferred to the photoelectron. When applying reverse bias, both electron and hole move along the electrical field drifting towards the multiplication area. This area consists of a regular doped p-layer and a highly doped n^+-layer where a high electric field strength prevails. Reaching this zone the photoelectron is accelerated strongly. Through collision with other atoms new electron hole pairs can be generated. Now, both the photoelectron and the secondary electrons can continue producing further electron hole pairs and so on. This exponential increase of charge carriers leads to an avalanche of electrons and holes. [3]

In figure 2.4 a SiPM cross section including the basic features is shown. The entrance window for incoming light is formed by a p-layer which is placed on top of an n-layer made out of silicon substrate. These layers form the avalanche zone. Each APD has an individual quenching resistor, which separates it from its neighboring diode. Together, they make up a microcell. The quenching resistor is necessary to stop the avalanche. After the avalanche breakdown has started, the produced electric current increases rapidly which is followed by the voltage de-energizing at the resistor until it's below the breakdown voltage. Then the diode can recharge again. The smaller the value of the resistor the faster the diode is recharged and sensitive to new incoming photons. However, the gain is limited with small values of the resistor. Every entrance window of the sensitive diode is topped with an antireflective layer to reduce any reflection light losses. [3, 4]

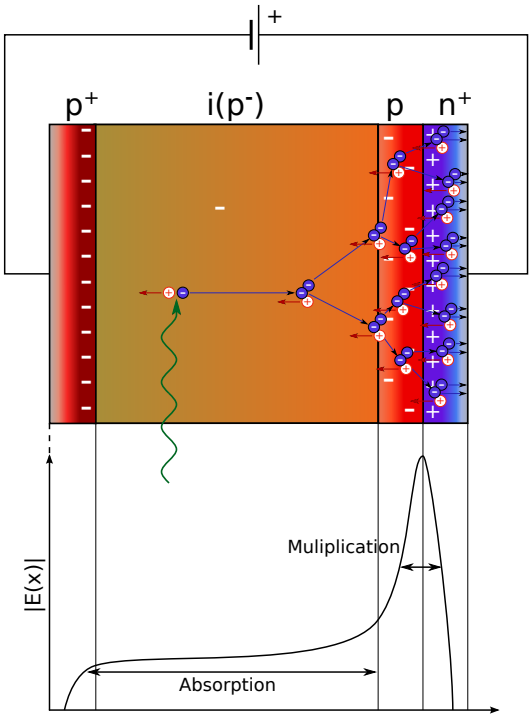

FIGURE 2.3: Schematic layout of an APD and its p^+-i-p-n^+ dopant profile. Below, the related strength of the electrical field is plotted. An avalanche process, created by an incoming photon with energy $E = h\nu$, is shown.

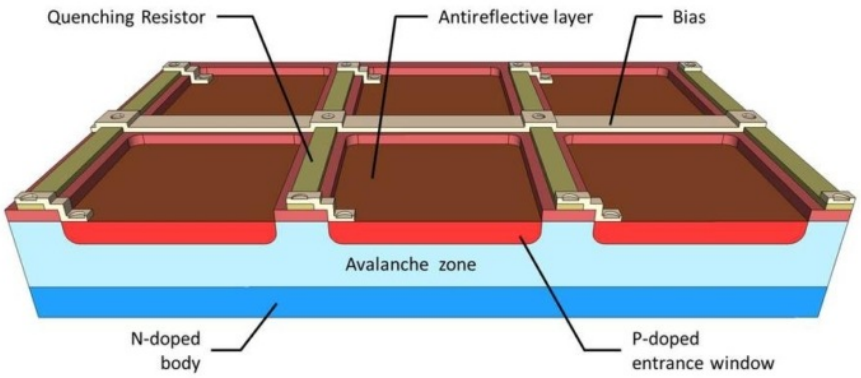

FIGURE 2.4: SiPM cross section scheme showing six pixels [4]. The entrance window consists of a highly doped p-layer placed on top of a silicon substrate and is topped with an antireflective layer. Each pixel is connected to a quenching resistor. External voltage is applied along the APDs.

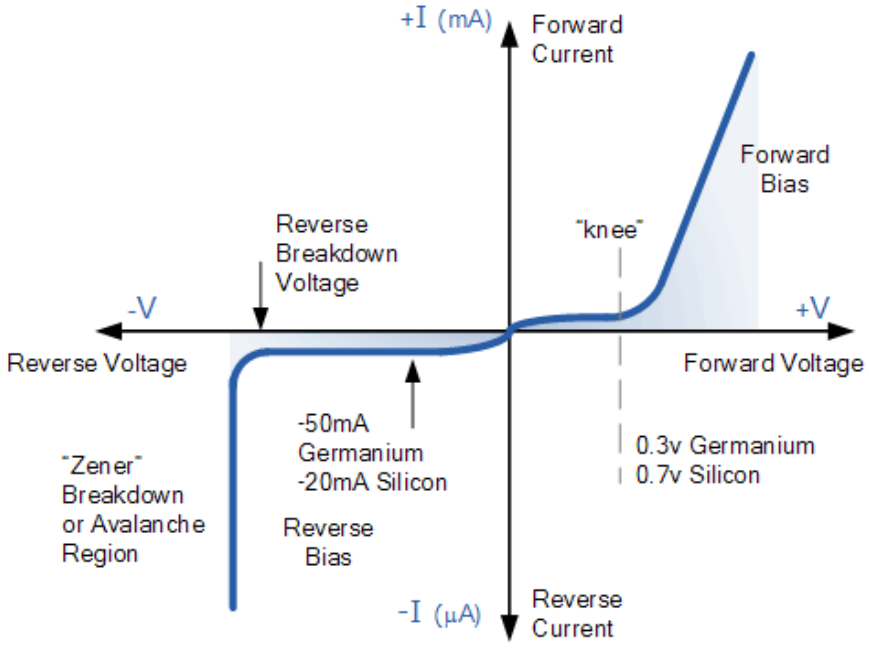

FIGURE 2.5: Schematic IV characteristics of a diode. Forward bias: cut-in voltage for silicon and germanium referred to as the "knee". Reverse bias: breakdown voltage and avalanche region. [5]

2.2 Diode Characteristics

When applying external voltage to a diode, its behavior varies depending on the sign and factor of the bias, which is shown in figure 2.5. In total, there are three possible methods in which a diode operates:

1. Zero Bias
2. Forward Bias
3. Reverse Bias

In a zero bias condition no external potential V_B is applied to the p-n junction. Nevertheless, if the terminals are shorted together, a few majority charge carriers move across the junction against the barrier potential. The forward current I_F is referred to when holes in the p-type section cross the p-n junction. In contrast, when holes which are created in the n-type (minority charge carriers) travel across the barrier in the opposite direction it is called reverse current I_R. This process also applies to free electrons only the other way around. Because of the potential

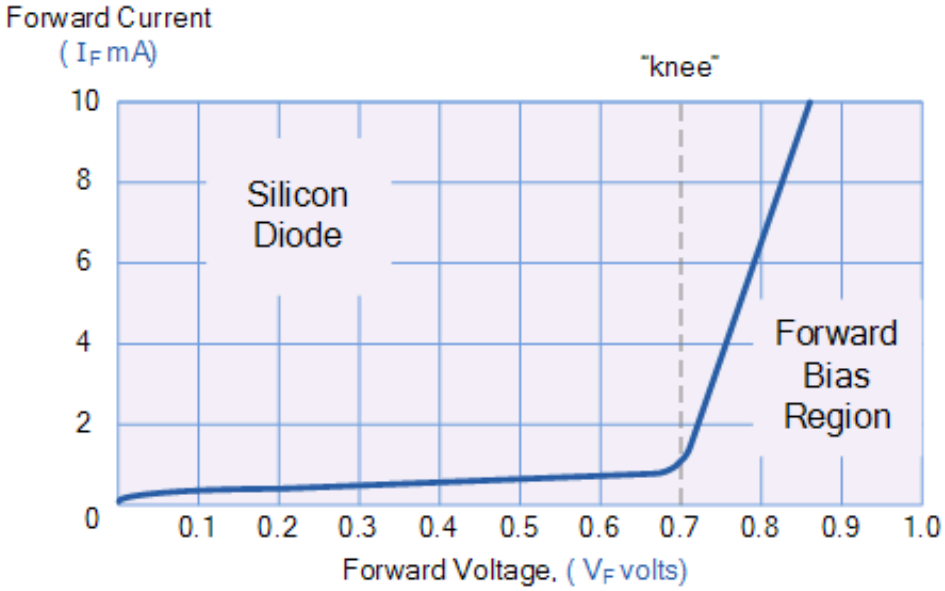

FIGURE 2.6: Schematic forward characteristics of a silicon diode. In the beginning, only a small electric current is able to flow because of the potential barrier. When the voltage increases, the depletion region is decomposed allowing a large electric current to flow. This point is referred to as the "knee". It is either called forward voltage V_F or cut-in voltage. [5]

barrier, the majority charge carriers are prevented from diffusing across the junction. However, minority charge carriers are still able to transfer back and forth until the state of the "Dynamic Equilibrium" is reached. In this state, diffusion is equal to drift resulting in zero net current. In conclusion, when $V_B = 0\,V$, no diode current is registered, $I_D = 0\,A$. [5]

Considering the forward bias condition, the positive terminal of a power supply is connected to the p-type semiconductor and the negative terminal to the n-type. The resulting IV characteristics is shown in figure 2.6. As long as the external voltage is below the potential barrier, only a small electric current will flow. However, when the bias is increased, it decomposes the barrier and the diode allows a large electric current to flow which increases rapidly with even small voltage boosts. For silicon this point is reached at about 0.7 V and for germanium at 0.3 V [5, 6]. This current is either called forward voltage V_F or cut-in voltage and is referred to as the "knee" in figure 2.5 and figure 2.6. The free electrons in the n-side are pushed towards and across the p-n junction by the negative terminal, where they recombine with the holes. This results in the reduction of the width of the depletion region, which leads to a reduced resistance by the depletion region and thus to an increase in electric current. The terminals are each responsible for supplying the p-side with

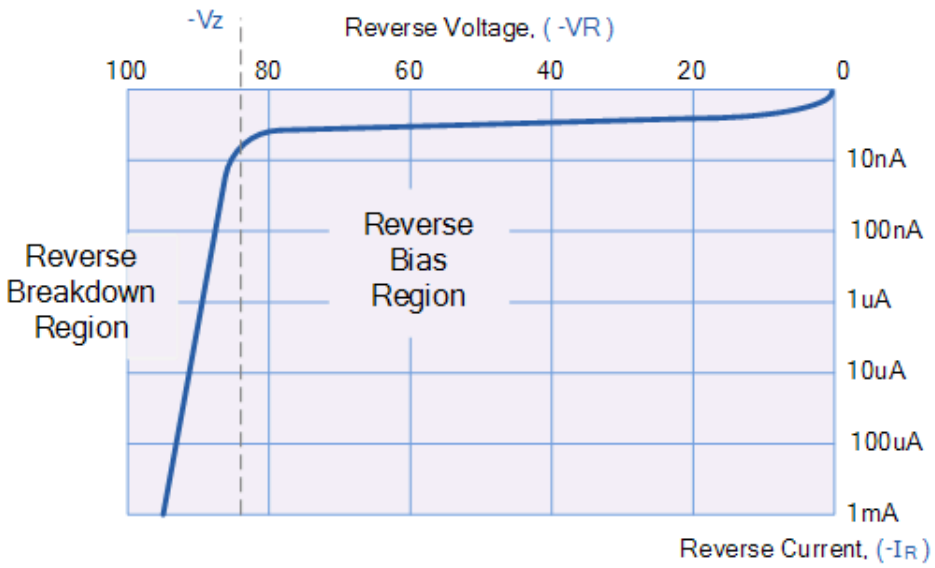

FIGURE 2.7: Schematic reverse characteristics of a silicon diode. For small bias only a small electric current occurs because the width of the depletion region blocks all the majority charge carriers from crossing the junction. The voltage at which the electric current increases rapidly is called breakdown voltage and is referred to as $-V_Z$. [5]

holes and the n-side with free electrons. In conclusion, the electric current increases with an increase in voltage. [5, 7]

Considering the reverse bias condition, the positive terminal is connected to the n-type semiconductor and the negative terminal to the p-type. The resulting IV characteristics is shown in figure 2.7. The holes in the p-side are attracted to the negative potential and move away form the p-n junction. Simultaneously, the free electrons in the n-side are attracted to the positive terminal and pulled away from the junction. This results in an increase of the width of the depletion region. The high potential barrier completely blocks the flow of majority charge carriers. When increasing the reverse bias, the depletion width expands because more free electrons and holes are pulled away from the p-n junction. Therefore, an increase in bias does not lead to an increase in electric current. Due to the fact that all minority charge carriers are pushed towards the junction, a small electric current occurs. This small electric current is called reverse saturation current and depends on the temperature. When the temperature rises, more minority carriers are generated and the reverse current increases. If the external voltage is increased and reaches a high enough value, avalanche breakdown will occur. This means that the electric current increases rapidly, allowing a maximum flow of charge carriers. This process

is shown in figure 2.7 as the steep downward bend which the graph makes. APDs are designed to work in this breakdown region.

2.3 Temperature Dependence

In order to measure the direct temperature of a SiPM, a temperature-dependent parameter, such as IV characteristics, is necessary. The Shockley equation describes the role of a p-n junction and is used to simulate IV characteristics of diodes and outline the connection between forward current and voltage [8]. The following equation is an extension of the Shockley equation by the resistance R.

$$I_{\mathrm{D}}(V_{\mathrm{B}}) = I_{\mathrm{S}}(T) \cdot \left(\exp\left(\frac{V_{\mathrm{B}} - R I_{\mathrm{D}}}{n V_{\mathrm{T}}} \right) - 1 \right) \tag{2.1}$$

The Shockley equation includes the diode current I_{D}, the scale current I_{S}, the external voltage or bias V_{B}, the resistor R, the thermal voltage V_{T} and the ideality factor n. Four variables in this equation are temperature-dependent: $I_{\mathrm{S}}, V_{\mathrm{T}}, n$ and R. The thermal voltage V_{T} is described by $V_{\mathrm{T}} = k_{\mathrm{B}}T/q_{\mathrm{e}}$ with the Boltzmann constant k_{B}, the temperature T and the electron charge q_{e}. The resistance is likewise temperature-dependent, which can be proven by $R_{\mathrm{T}} = R_0 + \Delta R$ and $\Delta R = \alpha \cdot \Delta T \cdot R_0$. In this case, R_0 is the value of the resistance before the temperature was increased, R_{T} is the value of the resistance after the temperature was increased, ΔR is the change of the value of the resistor, α is the temperature coefficient of the resistance's material and ΔT is the change in temperature. For the ideality factor n no temperature-dependent model has been established yet. Nevertheless, its temperature dependence has been verified experimentally in several publications [8, 9, 10].

Due to the above mentioned temperature dependencies of factors in the diode characteristics equation, one can expect the forward IV characteristics to be temperature-dependent as well. This result is used for the measurements carried out in this thesis.

3 Measurement Setup

Several different components were used for the measurements of IV characteristics at different temperatures, which were carried out for this thesis.

First of all, four different SiPMs were taken in order to compare their performance when applying forward bias. These SiPMs were:

1. LF2016 by FBK
2. PM3350 by Ketek
3. VUV3 by Hamamatsu
4. VUV4 by Hamamatsu

The SiPMs were connected to a preamplifier board, which intensifies the signal produced by the photomultiplier devices. The board with the installed SiPM was fastened to an optical table. This construction is shown in figure 3.1. A light tight box made out of synthetic material was placed over this setup. The corners, edges and holes on the top and bottom were sealed with black duck tape. This procedure was necessary as it was relevant to measure in complete darkness because only dark IV curves were of importance. The box with the following dimensions, $32\,\mathrm{cm} \times 30\,\mathrm{cm} \times 30\,\mathrm{cm}$, is shown in figure 3.2.

The voltage value where the current increases is referred to as the forward voltage V_F or the cut-in voltage. To measure forward IV characteristics and determine the shift in V_F at different temperatures, the black box was placed in a climatic chamber, model 1007C by the company Testequity [11]. It has an operation range from $-75\,^\circ\mathrm{C}$ to $75\,^\circ\mathrm{C}$, its workspace dimensions are about $60\,\mathrm{cm} \times 54\,\mathrm{cm} \times 60\,\mathrm{cm}$ and it has a stability of $\pm\,0.2\,^\circ\mathrm{C}$.

To reduce any incoming light, the viewing window in the front of the chamber was also sealed with black fabric. The adjustment of the temperature was done manually. It is important that the temperature is stable for the measurements to be at this precise temperature. In order to check the temperature stability,

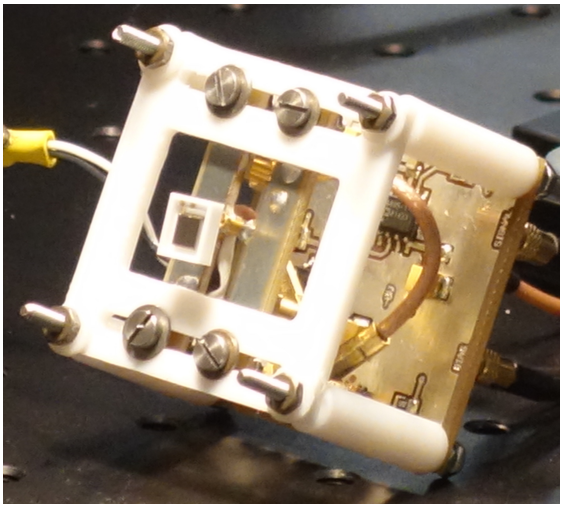

FIGURE 3.1: A SiPM is connected to a preamplifier board which is fastened to an optical table. A temperature sensor is attached to the preamplifier board as close as possible to the SiPM.

a temperature sensor was attached to the amplifier board as close as possible to the photomultiplier. The sensor was a film platinum resistance temperature detector (RTD) from the Honeywell HEL-700 series [12]. The sensor installed was a HEL-705 RTD with two wire contact and four wire readout. Its temperature accuracy is $\pm 0.5\,°C$. To record the temperature data, the sensor was connected to the computer via RedLab 3104 [13]. First it had to be configurated via the program InstaCal. Afterwards, the program TracerDAQPro was used to record the actual temperature.

The SiPMs were connected to a power supply and an ammeter in order to gather their data. The layout of the measurement setup is shown in figure 3.3. The power supply, used for forward biasing, was an Agilent E3631A Triple Outlet DC Power Supply [14]. Its stability is 0.02% of the output with an offset of 2 mV. Because the current output checkout wasn't accurate enough to read the very small leakage current in µA, an additional multimeter was used. This ammeter was a Fluke type 8845A/8846A [15] and was connected in series to the power supply. In order to hook up the preamplifier board to the output $\pm 25\,V$ and the mutual ground "common" of the power supply, the cables were lead through a cable duct in the climatic chamber, which was also sealed with duck tape. Both ammeter and voltage device were connected to a computer to record all measurement results.

For setting the external voltage and reading the diode current, a program was written in Python addressing both devices. First the external voltage was set and read, saving it in a file. Then the corresponding current was read ten times in order to observe its stability. After finishing one value of bias, the voltage was increased

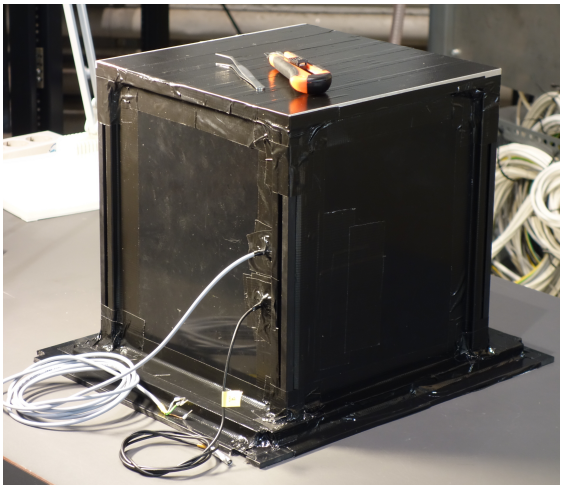

FIGURE 3.2: A light tight box made of synthetic material is placed on the optical table over the preamplifier board with installed SiPM inside. The gray RTD cable and the black bias cable are lead through holes in the box.

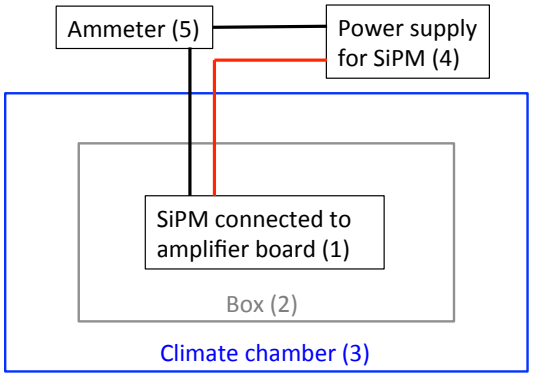

FIGURE 3.3: Schematic layout of the measurement setup. The SiPM which was connected to a preamplifier board was fastened to an optical table (1). To ensure complete darkness, a light tight box was placed over this setup (2). The black box was then placed in a climatic chamber (3). The SiPM was connected to a power supply (4) and an ammeter (5) in series.

by 0.01 V automatically and this process was rerun. The voltage was set from 0 V to 1 V in 0.01 V steps. When the voltage set points were completed, all the taken data was stored in a text file for further analysis. A current limit of 10^{-3} A was added as well, to stop any measurements in case such currents were reached before the program stopped at 1 V.

4 Data Analysis

4.1 Measurement Procedure

The measurements were carried out for nine different temperatures from $-70\,°C$ to $10\,°C$, starting at $10\,°C$ and continuing in steps of $10\,°C$. First of all, the temperature for an upcoming measurement was adjusted at the climatic chamber. The climatic chamber cools down the inner workspace to the desired temperature. It has a stability of about $0.2\,°C$. The actual temperature was recorded with the temperature sensor via the computer program TracerDAQPro. The measurements were started as soon as the fluctuation was about $0.2\,°C$ from the set point.

In order to determine diode IV characteristics, both voltage and current were measured by the multimeters. For each temperature, the voltage was varied in steps of $0.01\,V$. After the diode current was recorded 10 times for each bias, the average current was calculated and used for further analysis. Bias was set from $0\,V$ to $1\,V$ or until the current had reached $10^{-3}\,A$.

4.2 Calibration of IV Characteristics

The four different SiPMs were measured separately at room temperature. This was executed outside of the climatic chamber. The results for the first measurements are shown in figure 4.1. The figure shows the current in respect to the voltage. The graph reports typical forward IV characteristics of four SiPMs. The first part of the curve from $0\,V$ until the cut-in voltage is reached at the "knee" is the leakage current of the diode. As described in chapter 2, the width of the depletion region is reduced with increasing voltage, thus increasing the current flow. This is described in the area around the knee of the curve where the current starts to increase. The third part of the curve is dominated by the quenching resistor of the SiPM and therefore has a steady slope. This statement can be hinged on following equation:

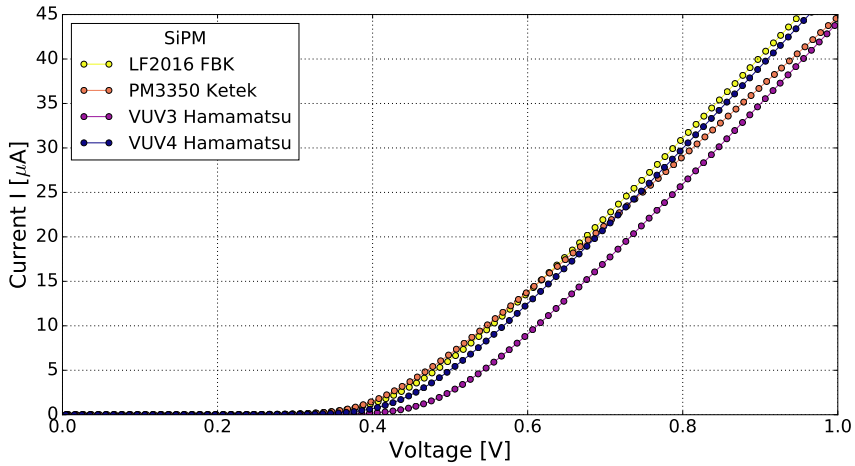

FIGURE 4.1: Forward IV characteristics of the four different SiPMs, LF2016 by FBK, PM3350 by Ketek, VUV3 by Hamamatsu and VUV4 by Hamamatsu, at room temperature are shown.

$$\frac{1}{R} = \frac{I}{U} \tag{4.1}$$

The slope of the curve is dependent on the inverse of the value of the quenching resistor R. An inner diode resistance also exists, which, however, is quite small. It can be noted that the gradient of the PM3350 Ketek SiPM is lower than the gradient of the other SiPMs. This probably has something to do with the different value of quenching resistors of the SiPMs, but cannot be said for certain, because no accurate description of the exact detection design is provided by the manufacturers.

For further temperature measurements, the SiPMs PM3350 by Ketek and VUV3 by Hamamatsu were used.

4.2.1 PM3350 by Ketek

The PM3350 SiPM by Ketek was placed in the climatic chamber to measure IV characteristics at different temperatures in the range of −70 °C to 10 °C, starting at 10 °C and continuing in steps of 10 °C. For each temperature the process described in section 4.1 was fulfilled. The data is shown in figure 4.2. Again, the very small leakage current at the beginning of the curve is recognizable. The graph shows that the cut-in voltage increases with decreasing temperature. Another thing, which stands out, is that the lower the temperature, the lower the forward current

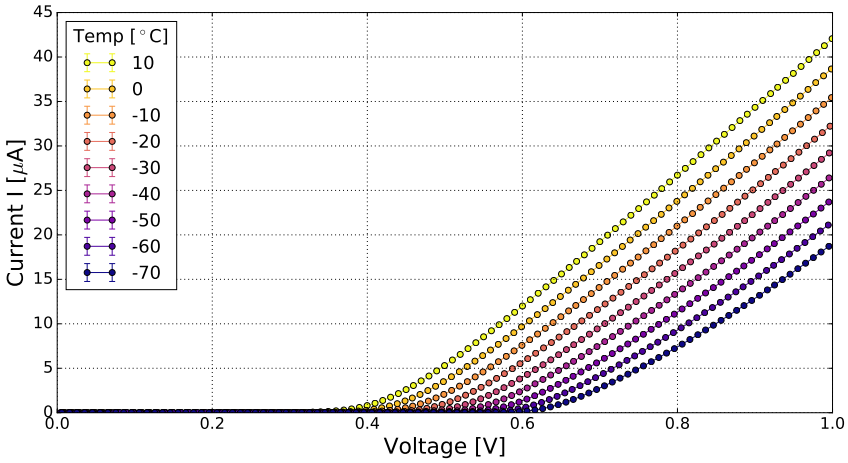

FIGURE 4.2: Forward IV characteristics of PM3350 by Ketek at different temperatures. The cut-in voltage increases with decreasing temperature. The slope of the curve decreases with decreasing temperature.

for any given voltage, meaning the curve is shifted to the right with decreasing temperature. It can also be observed that the lower the temperature, the smaller the gradient of the curve. Since the slope of the curve is proportional to R^{-1}, the resistor increases with decreasing temperature. This leads to the conclusion that the resistor dependent section of the curve is also temperature-dependent.

4.2.2 VUV3 by Hamamatsu

The VUV3 SiPM by Hamamastu, which was also selected, was placed in the climatic chamber to measure IV characteristics. The same temperature settings were taken as for the Ketek SiPM, and the same process as before was fulfilled for each temperature. The results are shown in figure 4.3. The cut-in voltage increases and the gradient of the curve decreases with decreasing temperature. It can be observed that the cut-in voltage of the VUV3 SiPM is generally higher than the cut-in voltage of the SiPM by Ketek, probably indicating a different diode or doping material or a different diode structure. Furthermore, the slope of the VUV3 curves is steeper than the slope of the curves of the Ketek SiPM. This fact is probably due to the different value of the quenching resistors of the SiPMs.

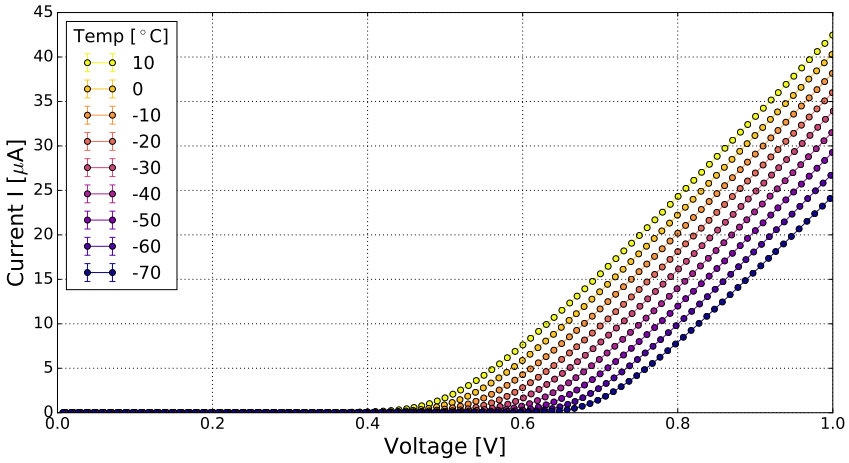

FIGURE 4.3: Forward IV characteristics of a VUV3 device by Hamamatsu at different temperatures. The cut-in voltage increases with decreasing temperature. The slope of the curve decreases with decreasing temperature.

4.3 Voltage-temperature Dependence

In order to determine the temperature at a certain voltage, the voltage-temperature dependence of the forward voltage at a given constant current value was extracted from the IV curves. A current of $I = 0.15\,\mu\text{A}$ was chosen. This area in the curve was enlarged and is shown in figure 4.4 for both SiPMs. In order to measure the area where the diode is in working mode, it is important that this current lies in the bend of the curve. If a too low current is chosen, the results of the leakage current where the diode isn't in working mode yet will be determined. If a too high current is chosen, it will lie in the resistance dependent region. This area is inconvenient because the quenching resistor produces heat which can affect the temperature measurement.

The determination of the voltage corresponding to the prescribed current was done with a linear interpolation of the two data points closest to $0.15\,\mu\text{A}$. In order to expand the voltage-temperature dependence towards lower temperatures than $-70\,°\text{C}$, a linear fit was applied to the existing data and extrapolation was done. Figure 4.5 shows the determined voltage at $0.15\,\mu\text{A}$ as a function of the temperature for both SiPMs. The fit, shown in the graph, is limited to certain temperatures, but can be adjusted to the temperatures needed. The temperature relevant for the setup in Erlangen lies between $-90\,°\text{C}$ and $-100\,°\text{C}$ for applications with liquid xenon. A temperature of $-95\,°\text{C}$ was picked to demonstrate the method in this thesis. The uncertainty of the voltage at this temperature was calculated based on

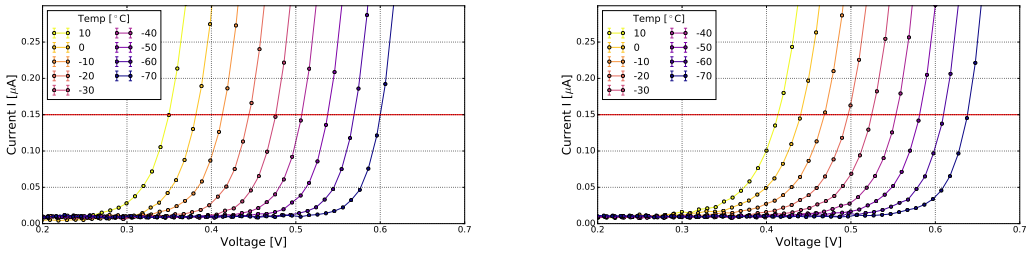

FIGURE 4.4: Zoom of the forward IV characteristics of PM3350 by Ketek (left) and VUV3 by Hamamatsu (right) at different temperatures in the range of −70 °C to 10 °C. An arbitrary current of $I = 0.15\,\mu\text{A}$ was chosen and is featured as the red horizontal line.

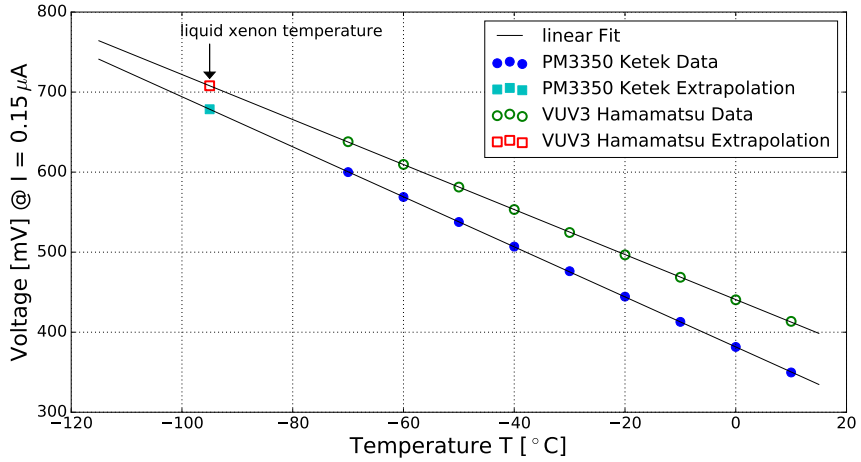

FIGURE 4.5: The voltage at 0.15 µA as a function of the temperature is shown for the PM3350 by Ketek and for the VUV3 by Hamamatsu. The blue dots represent the data of the PM3350 by Ketek and the cyan square the extrapolation with the value $V(-95\,°\text{C}) = 707.91 \pm 0.33\,\text{mV}$. The green dots represent the data of the VUV3 by Hamamatsu and the red square the extrapolation with the value $V(-95\,°\text{C}) = 768.55 \pm 0.34\,\text{mV}$.

the uncertainty of the linear fit parameters via Gaussian error propagation. The extrapolation results in a voltage of $V(-95\,°\text{C}) = 707.91 \pm 0.33\,\text{mV}$ at a prescribed current of 0.15 µA for the PM3350 and a voltage of $V(-95\,°\text{C}) = 678.55 \pm 0.34\,\text{mV}$ at 0.15 µA for the VUV3.

For testing the goodness of the linear fit, the chi squared χ^2 and reduced chi squared χ^2_{red} were calculated with following equations

$$\chi^2 = \sum_i \left(\frac{f(x_\text{i}) - y_\text{i}}{\sigma_\text{i}} \right)$$
$$\chi^2_{\text{red}} = \frac{\chi^2}{\text{DOF}} \tag{4.2}$$

where σ_i is the uncertainty of the determined voltage, $f(x_\text{i})$ the calculated voltage value via the fit, y_i the value of the determined voltage and DOF the number of degrees of freedom. The number of degrees of freedom is achieved when subtracting the number of fit parameters from the number of data points, which in this case results in DOF $= 9 - 2 = 7$. For the SiPM by Ketek, a chi-squared of $\chi^2 = 0.37$ and a reduced chi-squared of $\chi^2_{\text{red}} = 0.053$ have been derived. For the SiPM by Hamamatsu, a chi-squared of $\chi^2 = 0.36$ and reduced chi-squared of $\chi^2_{\text{red}} = 0.051$ have been derived. For both SiPMs χ^2_{red} is significantly less than one, stating the model is "over-fitting" the data or the uncertainty of the determined voltage is indicated too large. The uncertainty of the stability of the power supply, used for forward biasing, is probably overestimated using rather large possible stability bands with 0.02% of the output with an offset of 2 mV. Nevertheless, the linear model of the fit can be seen as an appropriate option for fitting the data points.

Comparing the linear fits of both SiPMs, as shown in figure 4.5, it should be noted that the determined voltage at 0.15 µA of the VUV3 device is slightly higher than the voltage of the PM3350. This is due to the fact that the cut-in voltage of the Hamamatsu SiPM is higher than the cut-in voltage of the Ketek SiPM. Also the slope of the curve of the PM3350 is steeper than the slope of the curve of the VUV3.

4.4 Application

As motivated in chapter 1, it is important to know the precise temperature at which a SiPM is operated in order to be able to account for various parameters that are temperature-dependent. By means of the method presented in this work, one is able to establish the actual temperature of the SiPM material itself. After the SiPMs are installed in the characterization setup, an IV characteristic in the area of 0.15 µA is measured. Afterwards the voltage at the specific current chosen for the IV

calibration in section 4.3 is determined. The corresponding temperature can easily be calculated for the given voltage via the voltage-temperature curve in figure 4.5, so that the SiPM functions as a thermometer for its direct temperature. This method can also be applied to other SiPMs and different temperatures as needed. The uncertainty of the voltage calculated in section 4.3 can be transferred back to the temperature via the applied fit, which results in a temperature resolution of $\Delta T = 0.1\,°\mathrm{C}$ for both SiPMs. This temperature resolution presents a sufficiently good accuracy of the detector temperature for the SiPM characterization efforts.

5 Conclusion

In this thesis a method for direct temperature measurement of SiPMs was developed. The method was applied to the SiPMs PM3350 by Ketek and VUV3 by Hamamatsu.

In order to obtain a voltage-temperature dependence, forward IV characteristics were measured for different temperatures in the range of $-70\,^{\circ}\mathrm{C}$ to $10\,^{\circ}\mathrm{C}$ in a climate chamber. As expected, the IV characteristics are temperature-dependent, revealing that the cut-in voltage increases with decreasing temperature for a specific current while the forward current decreases with decreasing temperature for a fixed voltage.

In order to gather the voltage-temperature behavior a current value was picked, which lies in the bend of the IV curve and is not yet dominated by the resistor. The corresponding voltage was determined and plotted as a function of the temperature. A linear fit was applied to the data points and extrapolated for lower temperatures down to $-110\,^{\circ}\mathrm{C}$ to obtain the voltage values in the liquid xenon temperature range. The uncertainty of the linear fit results in a temperature resolution of $\Delta T = 0.1\,^{\circ}\mathrm{C}$ for both SiPMs.

For future measurements a fit for the forward IV characteristics can be developed in order to directly calculate the voltage-temperature dependence and the value of several important parameters, such as the quenching resistor.

As mentioned in chapter 1, the goal of the setup at the ECAP which works with liquid xenon is to characterize SiPMs. For these temperature-dependent characterization efforts it is important to know the exact temperature at which a SiPM is operated. In conclusion it can be said that the developed method enables us to obtain the direct temperature and to use a SiPM as a thermometer.

Bibliography

[1] M. Mazzillo et al. Silicon Photomultiplier Technology at STMicroelectronics. *IEEE Transactions on Nuclear Science*, 56:2434–2442, August 2009.

[2] `http://www.physics-and-radio-electronics.com` [Accessed: 13.2.2018].

[3] Valeri Saveliev. Silicon Photomultiplier - New Era of Photon Detection. In Kim Ki Young, editor, *Advances in Optical and Photonic Devices*, Rijeka, 2010. InTech.

[4] `https://www.ketek.net/sipm/technology/` [Accessed: 13.2.2018].

[5] `https://www.electronics-tutorials.ws/diode/diode_3.html` [Accessed: 19.2.2018].

[6] H. Norde et al. The Schottky barrier height of the contacts between some rare earth metals (and silicides) and p type silicon. *Applied Physics Letters*, 38(11):865–866, 1981.

[7] `https://learn.sparkfun.com/tutorials/diodes/real-diode-characteristics` [Accessed: 7.3.2018].

[8] A. Foertig, J. Rauh, V. Dyakonov, and C. Deibel. Shockley equation parameters of p3ht:pcbm solar cells determined by transient techniques. *Phys. Rev. B*, 86:115302, Sep 2012.

[9] M.P. Deshmukh and J. Nagaraju. Measurement of silicon and gaas/ge solar cell device parameters. *Solar Energy Materials and Solar Cells*, 89(4):403 – 408, 2005.

[10] P. Singh, S.N. Singh, M. Lal, and M. Husain. Temperature dependence of i–v characteristics and performance parameters of silicon solar cell. *Solar Energy Materials and Solar Cells*, 92(12):1611 – 1616, 2008.

[11] `https://www.testequity.com` [Accessed: 22.2.2018].

[12] `https://sensing.honeywell.com` [Accessed: 7.3.2018].

[13] `http://www.meilhaus.de/infos/download/download-menu/download-redlab.htm` [Accessed: 7.3.2018].

[14] `https://edisciplinas.usp.br/pluginfile.php/2405092/mod_resource/content/1/Agilent_E3631%20Power%20Supply_Users_Guide%20%284%29.pdf` [Accessed: 15.11.2017].

[15] `http://www.pewa.de` [Accessed: 15.11.2017].

[16] N Otte. The Silicon Photomultiplier - A new device for High Energy Physics, Astroparticle Physics, Industrial and Medical Applications. January 2006.

[17] P. Buzhan et al. The Advanced Study of Silicon Photomultiplier. In M. Barone, E. Borchi, J. Huston, C. Leroy, P. G. Rancoita, P. Riboni, and R. Ruchti, editors, *Advanced Technology - Particle Physics*, pages 717–728, November 2002.

[18] I. Ostrovskiy et al. Characterization of Silicon Photomultipliers for nEXO. *IEEE Trans. Nucl. Sci.*, 62(4):1825–1836, 2015.

[19] D Renker and E Lorenz. Advances in solid state photon detectors. *Journal of Instrumentation*, 4(04):P04004, 2009.

[20] Judith Schneider. Charakterisierung von Siliziumphotomultipliern. Bachelorarbeit, Friedrich-Alexander-Universität Erlangen-Nürnberg, 2015.

[21] A. Ramilli. Characterization of SiPM: temperature dependencies.

[22] D. Sandoval. Characteristics of Silicon and Germanium Diodes. 2018.

[23] C. Piemonte et al. Characterization of the First Prototypes of Silicon Photomultiplier Fabricated at ITC-irst. *IEEE Transactions on Nuclear Science*, 54:236–244, 2007.

Acknowledgements

I have been fortunate to have wonderful and competent people in my life during the process of this thesis and would like to thank those individuals.

- My thanks go to **PD Dr. Thilo Michel** for his supervision and for introducing me to the field of astroparticle physics.
- I want to acknowledge **Prof. Dr. Gisela Anton** for giving me the opportunity to write my thesis at her department.
- I also want to express my sincere gratitude to **Micheal Wagenpfeil** for his guidance and assistance in the process of the measurements for this thesis and also for his encouragement and his expertise in every aspect.
- My special thanks go to **Tobias Ziegler**, not only for his honest feedback, but also for showing me interesting glimpses of a different field in physics and always patiently answering all my questions.
- I want to extend my thanks to **Sebastian Schmidt** for his help especially with Python and other technical difficulties but also for all the laughs and for cheering me up.
- Also I send a big thank you to each member of my whole **working group** for making me feel at home and for a wonderful atmosphere. Thank you for sharing your knowledge and for skilfully distracting me when I needed a break. It was so much fun working with you.
- Heartfelt thanks go to my **parents** for their never-ending support in all my decisions and for offering me all the possibilities.

Statutory Declaration

I declare that I have developed and written the enclosed Bachelor Thesis completely by myself, and have not used sources or means without declaration in the text. Any thoughts from others or literal quotations are clearly marked. The Bachelor Thesis was not used in the same or in a similar version to achieve an academic grading or is being published elsewhere.

Erlangen, April 9, 2018

Naomi Vogel